

Two-loop correction to the Higgs boson mass in the MRSSM

Philip Diessner^a, Jan Kalinowski^b, Wojciech Kotlarski^{a,b*} and Dominik Stöckinger^a

^aInstitut für Kern- und Teilchenphysik, TU Dresden, 01069 Dresden, Germany

^bFaculty of Physics, University of Warsaw, Pasteura 5, 02093 Warsaw, Poland

We present the impact of two-loop corrections on the mass of the lightest Higgs boson in the Minimal R-symmetric Supersymmetric Standard Model (MRSSM). These shift the Higgs boson mass up by typically 5 GeV or more. The dominant corrections arise from strong interactions, from the gluon and its $N = 2$ superpartners, the sgluon and Dirac gluino, and these corrections further increase with large Dirac gluino mass. The two-loop contributions governed purely by Yukawa couplings and the MRSSM λ, Λ parameters are smaller. We also update an earlier analysis [1], which showed that the MRSSM can accommodate the measured Higgs and W boson masses. Including the two-loop corrections increases the parameter space where the theory prediction agrees with the measurement.

1 Introduction

The recent discovery at the LHC of a particle consistent with the long sought Higgs boson seemingly completes the Standard Model (SM). The mass of the particle is measured with an astonishingly high accuracy of $m_H = 125.09 \pm 0.24$ GeV [2]. The precise determination of this mass is of paramount importance not only within the context of the Standard Model, but also for finding the path beyond it. In fact, a number of experimental observations suggest that the SM cannot be the ultimate theory and many theoretical scenarios for the beyond the SM physics (BSM) have been proposed in past decades. In some models of BSM, in particular in supersymmetric extensions of the SM, the Higgs boson mass can be predicted. However, the current experimental accuracy is far better than theoretical predictions for Higgs boson mass in any given model of BSM physics. From the point of view of theory, the best accuracy has been achieved in the minimal supersymmetric extension of the SM (MSSM), in which the discovery of the Higgs boson and the determination of its mass have given a new impetus to the theoretical efforts. The most recent improvements comprise the inclusion of leading three-loop corrections [3, 4], resummations of leading logarithms beyond the two-loop level [5, 6], inclusion of the external momenta of two-loop self-energies [7, 8], and the evaluation of the $\mathcal{O}(\alpha_t^2)$ -contributions in the complex MSSM [9, 10]. The MSSM two-loop corrections controlled by Yukawa couplings and α_s have been known for quite some time for the real MSSM (see the above references for an overview of the literature).

The absence of any direct signal of supersymmetric particle production at the LHC, and the observed Higgs boson mass of ~ 125 GeV being rather close to the upper value of ~ 135 GeV achievable in the MSSM, are a strong motivation to consider non-minimal SUSY scenarios. In fact, non-minimal SUSY models can lift the Higgs boson mass (at the tree level by new F - or D -term contributions or at the loop level from additional new states), which makes these models more natural by reducing fine-tuning. They can also weaken SUSY limits either by predicting compressed spectra, or by reducing the expected missing transverse energy, or by reducing production cross-sections. The comparison of the measured Higgs boson mass with the theoretically predicted values in any given model is therefore highly desirable. Although the theoretical calculations for the SM-like Higgs boson mass in such models are less advanced, progress is being made in the development of highly automated tools which greatly facilitate the computations in non-minimal SUSY models: SARAH [11–13] automatically

*Corresponding author.

generates spectrum generators similar to `SPheno` [14, 15]; `FlexibleSUSY` [16] automatically generates spectrum generators similar to `Softsusy` [17].

In a recent paper [1] we considered the MRSSM, a highly motivated supersymmetric model with continuous R-symmetry [18, 19] distinct from the MSSM. Since R-symmetry forbids soft Majorana gaugino masses as well as the higgsino mass term, additional superfields are needed. The MRSSM has been constructed in Ref. [20] as a minimal viable model of this type. It contains adjoint chiral superfields with R-charge 0 for each gauge sector and two additional Higgs weak iso-doublet superfields with R-charge 2. Interestingly, R-symmetry also forbids large contributions to CP- and flavor-violating observables [20, 21], so the MRSSM is generically in agreement with flavor data even for an anarchic flavor structure in the sfermion sector and for sfermion masses below the TeV scale. Also, Dirac gluinos suppress the production cross-section for squarks, making squarks below the TeV scale generically compatible with LHC data. Furthermore, models with R-symmetry and/or Dirac gauginos contain promising dark matter candidates [22–24], and the collider physics of the extra, non-MSSM-like states has been studied [25–33].

In Ref. [1] the complete next-to-leading order computation and discussion of the lightest Higgs boson and W boson masses has been performed (a similar analysis has been done in Ref. [34]). We showed that the model can accommodate measured values of these observables for interesting regions of parameter space with stop masses of order 1 TeV. The outcome of the paper was not obvious since in the MRSSM (i) the lightest Higgs boson tree-level mass is typically reduced compared to the MSSM due to mixing with additional scalars, (ii) the stop mixing is absent and (iii) R-symmetry necessarily introduces an SU(2) scalar triplet, which can increase m_W already at the tree level. Nevertheless, we identified benchmark points BMP1, BMP2 and BMP3 illustrating different viable parameter regions for $\tan\beta = 3, 10, 40$ respectively, and also verified that they are not excluded by further experimental constraints from Higgs observables, collider and low-energy physics.

These promising results motivate a more precise computation of the Higgs boson mass in the MRSSM and a more precise parameter analysis. Technically, this is facilitated by the Mathematica package `SARAH`, recently updated by providing `SPheno` routines, which calculate two-loop corrections to the CP-even Higgs scalars masses in the effective potential approximation and the gaugeless limit [35]. This is the level of precision of the established MSSM predictions except for the refinements mentioned above. It is also the level of precision at which the proof [36] applies that the employed regularization by dimensional reduction preserves supersymmetry. First applications of the improved `SARAH` version to the calculations of the Higgs boson masses in the R-parity violating MSSM [37] and next-to-minimal SSM [38] have been published.

Since in [1] a judicious choice of the model parameters was needed to meet experimental constraints, and an estimate of unknown two-loop contributions was presented, it is of immediate interest to verify our findings at higher precision with the new `SARAH` version. The aim of the current paper is to calculate two-loop corrections for the Higgs boson mass in the MRSSM and present an update of the results obtained in [1].

The paper is organized as follows. After a short recapitulation of the MRSSM in section 2, we explain in section 3 our calculation framework and discuss the dependence of two-loop corrections on parameters that entered already at the one-loop level. The dependence on parameters that enter only at the two-loop level is investigated in section 4. In section 5 we provide an update to the analysis presented in [1] using the two-loop corrected masses of Higgses, before concluding in section 6.

2 The MRSSM

The MRSSM has been constructed in Ref. [20] as a minimal supersymmetric model with unbroken continuous R-symmetry. The superpotential of the model reads as

$$\begin{aligned}
W = & \mu_d \hat{R}_d \cdot \hat{H}_d + \mu_u \hat{R}_u \cdot \hat{H}_u + \Lambda_d \hat{R}_d \cdot \hat{T} \hat{H}_d + \Lambda_u \hat{R}_u \cdot \hat{T} \hat{H}_u \\
& + \lambda_d \hat{S} \hat{R}_d \cdot \hat{H}_d + \lambda_u \hat{S} \hat{R}_u \cdot \hat{H}_u - Y_d \hat{d} \hat{q} \cdot \hat{H}_d - Y_e \hat{e} \hat{l} \cdot \hat{H}_d + Y_u \hat{u} \hat{q} \cdot \hat{H}_u,
\end{aligned} \tag{1}$$

where $\hat{H}_{u,d}$ are the MSSM-like Higgs weak iso-doublets, and \hat{S} , \hat{T} , $\hat{R}_{u,d}$ are the singlet, weak iso-triplet and \hat{R} -Higgs weak iso-doublets, respectively. The usual MSSM μ -term is forbidden; instead the $\mu_{u,d}$ -terms involving R-Higgs fields are allowed. The Λ, λ -terms are similar to the usual Yukawa terms, where the \hat{R} -Higgs and \hat{S} or \hat{T} play the role of the quark/lepton doublets and singlets.

The usual soft mass terms of the MSSM scalar fields are allowed just like in the MSSM. In contrast, A -terms and soft Majorana gaugino masses are forbidden by R-symmetry. The fermionic components of the chiral adjoints, $\hat{\Phi}_i = \hat{O}, \hat{T}, \hat{S}$ for each standard model gauge group $i = SU(3), SU(2), U(1)$ respectively, are paired with standard gauginos $\tilde{g}, \tilde{W}, \tilde{B}$ to build Dirac fermions and the corresponding mass terms. The Dirac gaugino masses generated by D-type spurions produce additional terms with the auxiliary \mathcal{D} -fields in the Lagrangian,

$$V_D = M_B^D (\tilde{B} \tilde{S} - \sqrt{2} \mathcal{D}_B S) + M_W^D (\tilde{W}^a \tilde{T}^a - \sqrt{2} \mathcal{D}_W^a T^a) + M_g^D (\tilde{g}^a \tilde{O}^a - \sqrt{2} \mathcal{D}_g^a O^a) + \text{h.c.}, \quad (2)$$

which after being eliminated through their equations of motion, lead to the appearance of Dirac masses in the scalar sector as well. The soft-breaking scalar mass terms read

$$\begin{aligned} V_{SB}^{EW} = & m_{H_d}^2 (|H_d^0|^2 + |H_d^-|^2) + m_{H_u}^2 (|H_u^0|^2 + |H_u^+|^2) + [B_\mu (H_d^- H_u^+ - H_d^0 H_u^0) + \text{h.c.}] \\ & + m_{R_d}^2 (|R_d^0|^2 + |R_d^+|^2) + m_{R_u}^2 |R_u^0|^2 + m_{R_u}^2 |R_d^-|^2 \\ & + m_S^2 |S|^2 + m_T^2 |T^0|^2 + m_T^2 |T^-|^2 + m_T^2 |T^+|^2 + m_O^2 |O|^2 \\ & + \tilde{d}_{L,i}^* m_{q,ij}^2 \tilde{d}_{L,j} + \tilde{d}_{R,i}^* m_{d,ij}^2 \tilde{d}_{R,j} + \tilde{u}_{L,i}^* m_{q,ij}^2 \tilde{u}_{L,j} + \tilde{u}_{R,i}^* m_{u,ij}^2 \tilde{u}_{R,j} \\ & + \tilde{e}_{L,i}^* m_{l,ij}^2 \tilde{e}_{L,j} + \tilde{e}_{R,i}^* m_{e,ij}^2 \tilde{e}_{R,j} + \tilde{\nu}_{L,i}^* m_{l,ij}^2 \tilde{\nu}_{L,j}. \end{aligned} \quad (3)$$

The electroweak symmetry breaking (EWSB) is triggered by non-zero vacuum expectation values of the $R = 0$ neutral EW scalars, which are parameterized as

$$\begin{aligned} H_d^0 &= \frac{1}{\sqrt{2}} (v_d + \phi_d + i\sigma_d), & H_u^0 &= \frac{1}{\sqrt{2}} (v_u + \phi_u + i\sigma_u), \\ T^0 &= \frac{1}{\sqrt{2}} (v_T + \phi_T + i\sigma_T), & S &= \frac{1}{\sqrt{2}} (v_S + \phi_S + i\sigma_S); \end{aligned}$$

R-Higgs bosons carry R-charge 2 and therefore do not develop vacuum expectation values. We stress that in general the mixing of ϕ_T, ϕ_S with ϕ_u and ϕ_d leads to a reduction of the lightest Higgs boson mass at the tree-level compared to the MSSM.

3 Higgs mass dependence on the λ, Λ superpotential parameters

We now present the MRSSM Higgs boson mass prediction at the two-loop level. We use the same renormalization scheme as in Ref. [1], where all SUSY parameters are defined in the $\overline{\text{DR}}$ scheme and $m_{H_d}^2, m_{H_u}^2, v_S$ and v_T are determined by minimizing the effective potential at the two-loop order. The discussion is divided into two parts. In the present section we begin with the one-loop contributions, which are dominated by terms of $\mathcal{O}(\alpha_{t,b,\lambda})$, where α_λ collectively denotes squares of the superpotential couplings $\lambda_{u,d}$ and $\Lambda_{u,d}$. We then discuss the two-loop contributions of $\mathcal{O}(\alpha_{t,b,\lambda}^2)$, i.e. ones which depend on parameters which already play a role at the one-loop level. In the subsequent section we then discuss those two-loop corrections which involve new parameters.

In the usual MSSM, the one-loop contributions to the Higgs boson mass are dominated by top/stop contributions. In the MRSSM, these contributions are also important, but they are simpler since stop mixing is forbidden by R-symmetry (corresponding to the MSSM parameter $X_t \equiv A_t - \mu/\tan\beta = 0$). This implies that the top/stop contributions cannot reach values as high as in the MSSM for a given stop mass scale. However, as mentioned above, the MRSSM superpotential contains new terms governed by $\lambda_{u,d}$ and $\Lambda_{u,d}$ which have a Yukawa-like structure. References [1, 34] have given a useful analytical approximation for these contributions. In the the limit $\lambda = \lambda_u = -\lambda_d, \Lambda = \Lambda_u = \Lambda_d, v_S \approx v_T \approx 0$ and

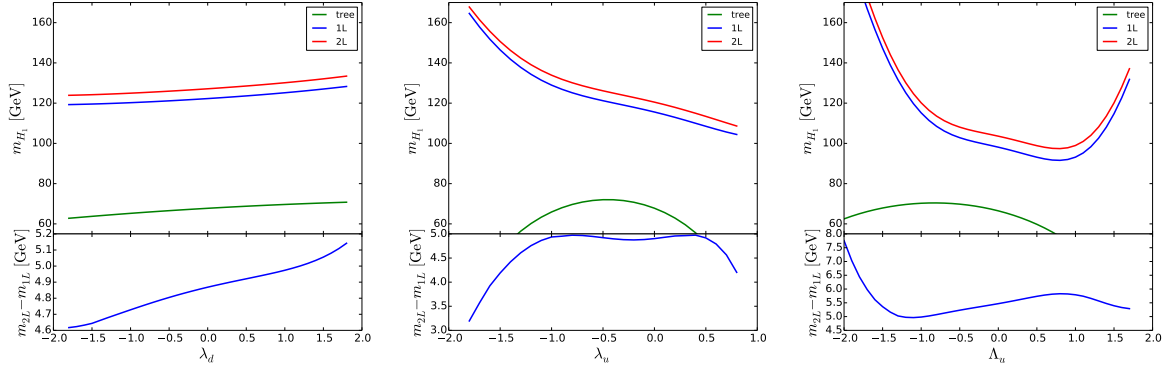


Figure 1: Lightest MRSSM Higgs boson mass m_{H_1} , and the difference $m_{2L} - m_{1L}$ between masses calculated at the two-loop and one-loop level, as a function of λ_d , λ_u , Λ_u , respectively. In the upper parts of the figure lines from top to bottom correspond to two-loop, one-loop and tree level calculations. All other parameters are set to the values of benchmark point BMP1 with $\tan \beta = 3$ (see Tab. 2).

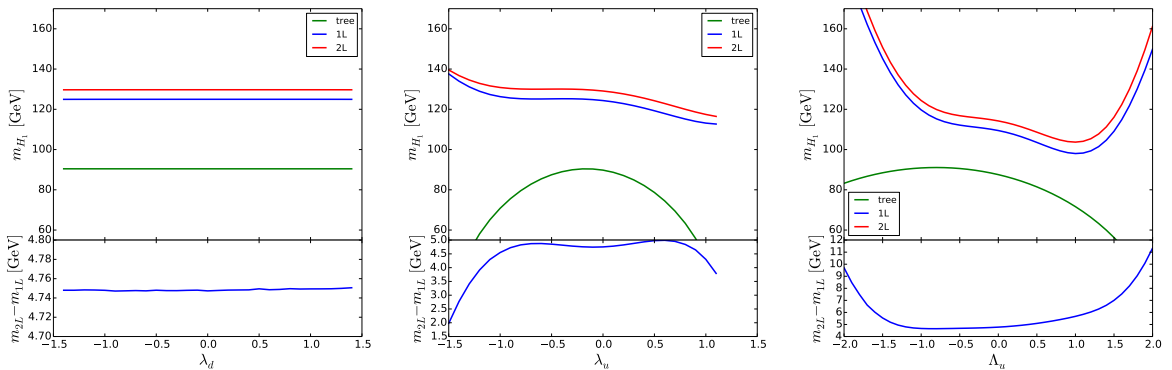


Figure 2: As in Fig. 1, but for benchmark point BMP3 with $\tan \beta = 40$ (see Tab. 2).

large $\tan \beta$, we get

$$\begin{aligned}
\Delta m_{H_1, \text{eff.pot}, \lambda}^2 = & \frac{2v^2}{16\pi^2} \left[\frac{\Lambda^2 \lambda^2}{2} + \frac{4\lambda^4 + 4\lambda^2 \Lambda^2 + 5\Lambda^4}{8} \log \frac{m_{R_u}^2}{Q^2} \right. \\
& + \left(\frac{\lambda^4}{2} - \frac{\lambda^2 \Lambda^2}{2} \frac{m_S^2}{m_T^2 - m_S^2} \right) \log \frac{m_S^2}{Q^2} + \left(\frac{5}{8} \Lambda^4 + \frac{\lambda^2 \Lambda^2}{2} \frac{m_T^2}{m_T^2 - m_S^2} \right) \log \frac{m_T^2}{Q^2} \\
& \left. - \left(\frac{5}{4} \Lambda^4 - \lambda^2 \Lambda^2 \frac{(M_W^D)^2}{(M_B^D)^2 - (M_W^D)^2} \right) \log \frac{(M_W^D)^2}{Q^2} - \left(\lambda^4 + \lambda^2 \Lambda^2 \frac{(M_B^D)^2}{(M_B^D)^2 - (M_W^D)^2} \right) \log \frac{(M_B^D)^2}{Q^2} \right]. \quad (4)
\end{aligned}$$

This result shows a behavior proportional to λ^4 , Λ^4 and $\log m_{\text{soft}}^2$. This is similar to the top/stop contributions as the λ 's and Y_t appear in a similar fashion in superpotential.

We expect therefore that the two-loop result will depend on these model parameters (which already entered at the one-loop level) in a manner similar to the pure top quark/squarks two-loop contributions, i.e. similar to the MSSM $\mathcal{O}(\alpha_t^2)$ contributions without stop mixing.

In Figs. 1 and 2 the dependence of the lightest Higgs boson mass calculated at tree-, one- and two-loop levels for two benchmarks BMP1 and BMP3 on different model parameters is shown. All parameters except the ones shown on the horizontal axes are set to the values of the benchmark points defined in Ref. [1] (see Tab. 2). Indeed the λ, Λ behavior of the two-loop corrections is very similar to the one of the corresponding one-loop corrections. The numerical impact of the two-loop λ, Λ -contributions is rather small, typically less than 1 GeV, except for very large $|\lambda_u|, |\Lambda_u| > 1$, where they can reach several GeV. Particularly, the strong λ_u dependence for large λ_u is already manifest for the

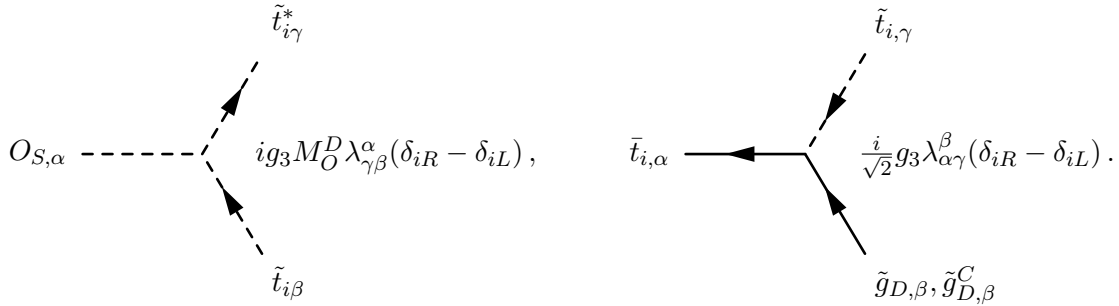


Figure 3: Feynman rules needed to evaluate diagrams of Fig. 4. In the right diagram, the charge-conjugated gluino $\tilde{g}_{D,\beta}^C$ applies in the case of $i = L$, $\tilde{g}_{D,\beta}$ in the case of $i = R$.

tree-level mass; this is due to the mixing with the singlet state already present in the tree-level mass matrix.

One should remember that very large one-loop contributions are required to bring the predicted Higgs boson mass close to the experimental one. In the preferred parameter regions, the λ, Λ are large but still moderate enough not to blow up the two-loop contributions.

Overall, the total two-loop contributions (including the ones to be discussed in the subsequent section) are in the range between 4 and 5 GeV, except in the very large λ, Λ regions. This is in agreement with the estimate given in Ref. [1], and it confirms the validity of the perturbative expansion in spite of the large one-loop corrections.

4 QCD corrections and the two-loop corrected Higgs boson mass

At two-loop level the strongly interacting sector and the strong coupling α_s appear directly in the Higgs boson mass predictions. These two-loop corrections involve not only the gluon but also the Dirac gluino and the sgluon, the scalar component of the octet superfield \hat{O} . They can be expected to be sizable, and they depend on the gluino Dirac mass and sgluon soft mass parameters.¹ The gluino Dirac mass parameter M_O^D appears not only directly as the gluino mass but, via Eq. (2), also in couplings and mass terms of sgluons, inducing the mass splitting² between the real and imaginary parts of the sgluon field, $O = \frac{1}{\sqrt{2}}(O_S + iO_A)$. The masses of the scalar sgluons O_S and pseudoscalar sgluons O_A are related by the tree-level formula $m_{O_S}^2 = 4(M_O^D)^2 + m_{O_A}^2$, where $m_{O_A}^2$ is equal to the soft-breaking parameter m_O^2 [25, 27]. The relevant vertices and Feynman rules are depicted in Fig. 3. We assume real M_O^D , so only the scalar O_S acquires the direct coupling to sfermions proportional to M_O^D , via Eq. (2).

The structure of the strong corrections is thus markedly different from the MSSM case, where only the Majorana gluino and the gluon appear. In the following, we study the magnitude and the behavior of the corrections as a function of the parameters M_O^D and m_O^2 .

4.1 Analytic formulas

As in the previous section, we begin with an analytic approximation for the leading contributions of $\mathcal{O}(\alpha_t \alpha_s)$, i.e. two-loop strong corrections proportional to Y_t^2 . This provides us with qualitative insight and serves as a check of the code. Generally, in the gaugeless limit the two-loop corrections from gluinos and sgluons contribute only to the diagonal part of the $\{\phi_d, \phi_u\}$ submatrix of the scalar Higgs boson mass matrix. In the MRSSM the $\mathcal{O}(\alpha_t \alpha_s)$ terms contribute only to the $\phi_u \phi_u$ element. This

¹ These parameters already play a role at lower order, appearing in corrections to Y_t (through threshold corrections to $\hat{\alpha}_s$), though the influence on, for example, DR top mass is negligible.

²In Ref. [1] a simplifying assumption was made that masses of the scalar and pseudoscalar components of (complex) sgluon field were equal, since it was unimportant for that analysis.

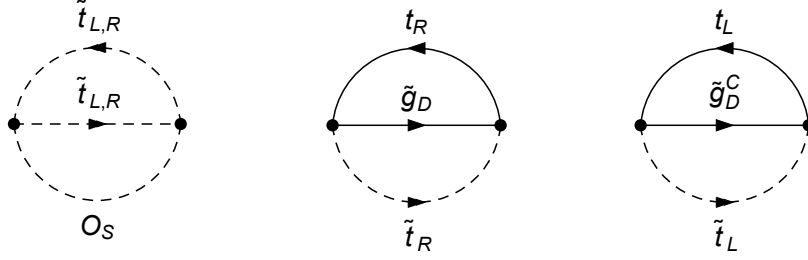


Figure 4: Two-loop diagrams contributing to the Higgs boson mass via Eq. (5) that depend on the Dirac mass M_O^D and the soft sgluon mass m_O . We only draw diagrams involving top/stop; similar diagrams exist for all quark/squark flavors.

already constitutes a difference to the MSSM, where the μ -term violates R-symmetry and Peccei-Quinn symmetry leading to couplings of stops to ϕ_d .

Figure 4 shows two-loop diagrams contributing to the Higgs boson mass at $\mathcal{O}(\alpha_t\alpha_s)$ that explicitly depend on m_O and/or M_O^D . These diagrams provide the following contribution to the effective potential:

$$V_{eff}^{(2)} = \frac{8g_3^2}{(16\pi^2)^2}(M_O^D)^2 \sum_{i=L,R} f_{SSS}(m_{\tilde{t}_i}^2, m_{\tilde{t}_i}^2, m_{O_S}^2) + \frac{8g_3^2}{(16\pi^2)^2} \sum_{i=L,R} f_{FFS}(m_t^2, m_{\tilde{t}_i}^2, m_{\tilde{g}_D}^2), \quad (5)$$

where the functions f_{SSS} and f_{FFS} are defined in [39]. The effective potential $V_{eff}^{(2)}$ depends on v_u through stop masses, which in the gaugeless limit approach

$$m_{\tilde{t}_L\tilde{t}_L}^2 \rightarrow m_q^2 + \frac{1}{2}Y_t^2 v_u^2, \quad (6)$$

$$m_{\tilde{t}_R\tilde{t}_R}^2 \rightarrow m_u^2 + \frac{1}{2}Y_t^2 v_u^2. \quad (7)$$

Equation (5) can be obtained from Ref. [39] by applying translation rules from real fields to complex ones. Many such rules can be found in Ref. [35]; an additional rule needed here for the case of a Lagrangian $\mathcal{L} \ni -c\Phi_1|\Phi_2|^2$, where $\Phi_1, c \in \mathbb{R}$, $\Phi_2 \in \mathbb{C}$, is $V_{SSS} = \frac{1}{2}|c|^2 f_{SSS}(m_1^2, m_2^2, m_2^2)$.

An important difference to the MSSM is that contributions with fermion mass insertions, corresponding to \overline{FFS} -type contributions in Ref. [39], are not present in the MRSSM. Such contributions vanish due to the lack of L-R mixing between squarks. Hence the gluino mass appears in a simpler way than in the MSSM. Likewise, the sgluon only enters via the SSS -type diagram of Fig. 4. An SS -type diagram vanishes due to the color structure.

The corresponding two-loop contribution to the $\phi_u\phi_u$ Higgs boson mass matrix element in zero-momentum approximation is then given by³

$$[\Delta m_{H_1}^2]_{\phi_u\phi_u} = \left(\frac{\partial^2}{\partial v_u \partial v_u} - \frac{1}{v_u} \frac{\partial}{\partial v_u} \right) V_{eff}^{(2)}. \quad (8)$$

For large $\tan\beta$, corrections of order $\mathcal{O}(\alpha_b\alpha_s)$ cannot be neglected any more. But since they contribute only to $\phi_d\phi_d$ matrix element, their impact on mass of the lightest Higgs, which stems mainly from the $\phi_u\phi_u$ element, is small. Results of Eq. (5) were compared with the results of two-loop routines from the SARAH-generated SPheno module.

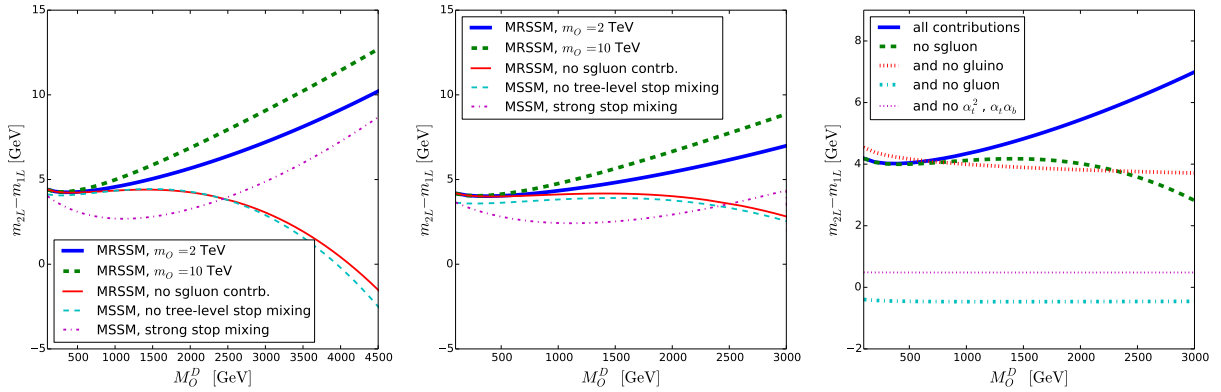


Figure 5: Two-loop contributions to the SM-like Higgs boson mass depending on the gluino mass in the MRSSM for BMP1 (left panel) and BMP3 (middle panel) and two different values of the soft sgluon mass parameter $m_O = 2$ TeV (thick solid blue line) and 10 TeV (thick dashed green line) with all contributions, respectively, and without the sgluon contributions (thin solid red line). For comparison also the MSSM contributions for no (thin dashed light blue line) and maximal (purple dotted line) stop mixing are plotted. The chosen MSSM parameters are given in Tab. 1. For BMP3 and $m_O = 2$ TeV the right panel shows the result, when successively switching off dominating and sub-dominating contributions.

	$\tan \beta$	M_1	M_2	μ	m_A	$m_{q,u,d;(3,3)}^2$	$m_{q,u,d}^2$	$m_{l,e}^2$	$A_{\tau,b}$	X_t
left panel	3	600	500	400	700	1000^2	2000^2	1000^2	0	0/2000
right panel	40	250	500	400	700	1000^2	2000^2	1000^2	0	0/2000

Table 1: Definition of the fixed parameters for the MSSM points in Fig. 5. All parameters in GeV or GeV^2 , where appropriate. The stop mixing parameter X_t is given both for the cases of no and large stop mixing.

4.2 Numerical analysis

We now turn to the numerical analysis of the complete two-loop corrections to the SM-like Higgs boson mass, using the full evaluation within the framework of **SARAH** and **SPheno**. The first two panels of Fig. 5 focus on the gluino and sgluon mass dependence, which arises mainly from the $\mathcal{O}(\alpha_t \alpha_s)$ corrections; they show the two-loop corrections as a function of the gluino mass parameter for two different values of the soft sgluon mass, $m_O = 2$ and 10 TeV for two benchmarks BMP1 and BMP3; other parameters are fixed at benchmark values. For comparison, the two-loop result without the sgluon contribution is shown as well (i.e. without the first diagram of Fig. 4). We also plot the MSSM prediction with strong stop mixing and without any sfermion mixing the at tree-level.

The first two panels show that the dependence in the MRSSM without sgluon contributions is very similar to the one in the MSSM without stop mixing. The corresponding thin solid red and thin dashed light blue curves in Fig. 5 show a characteristic drop for large gluino masses. This is understandable as in the MSSM without sfermion mixing the gluino contribution is precisely the same as in the MRSSM and given by the two corresponding diagrams in Fig. 4. The Dirac or Majorana nature of the gluino does not matter since the Dirac partner, the octet superfield \hat{O} has no direct couplings to quark superfields. A few TeV gluino masses slightly increase the Higgs boson mass, but for larger values of M_O^D the f_{FFS} function becomes negative and drives the correction downwards.

In the full MRSSM calculations, including the sgluon diagrams strongly changes the behavior.

³As pointed out in [35], in **SARAH** and **SPheno** the two-loop tadpole contributions are included directly in vacuum minimization condition and not in Eq. 8.

Surprisingly, the full MRSSM two-loop contributions resemble the MSSM contributions with large stop mixing. In both cases, large gluino masses strongly enhance the Higgs boson mass, however for different reasons. In the MSSM the increase can be traced back to the additional $\overline{F}FS$ -type diagram which is directly proportional to M_O^D and which vanishes in the limit of no stop-mixing. In the MRSSM, on the other hand, the sgluon diagram grows with M_O^D both due to the sgluon-stop-stop coupling, which scales like M_O^D , and to an increase in the scalar (but not pseudoscalar) sgluon mass. Due to the sgluon contributions the total two-loop contributions to the Higgs boson mass in the MRSSM are larger than the ones in the MSSM. They are further increased by heavy sgluons.

The third panel of Figure 5 compares the numerical impact of individual contributions by successively switching off contributions. It allows to read off the contributions from sgluon, gluino and gluon, of $\mathcal{O}(\alpha_t^2, \alpha_t \alpha_b)$, and the remaining two-loop contributions (particularly the λ, Λ contributions). The gluon diagrams alone contribute approximately +4 GeV. The negative gluino and the positive sgluon corrections together amount to an additional upward shift of the Higgs boson mass, which can reach several GeV for large Dirac gluino masses. The remaining contributions are far smaller and amount to around -1 GeV for the $\mathcal{O}(\alpha_t^2, \alpha_t \alpha_b)$ contributions and +0.5 GeV for the remaining contributions.

5 Update of benchmarks

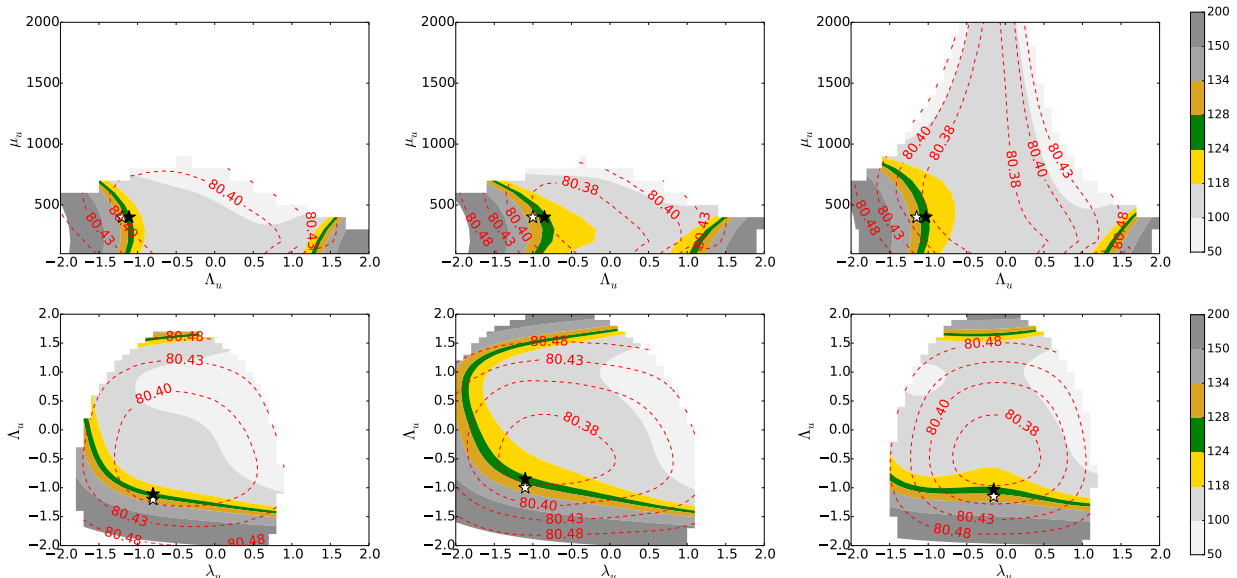


Figure 6: Contour plots showing the behavior of m_{H_1} given by the color map and m_W given by the red contour lines. The plots are ordered horizontally by benchmark points (top row for BMP1, bottom row for BMP3), while vertically different combinations of model parameters are varied. The white stars mark the original benchmark points from Ref. [1], whereas the black ones show the adapted points after taking into account the two-loop corrections.

In this section we present an update of the analysis of Ref. [1], using the more precise evaluation of the Higgs boson mass. Ref. [1] studied the mass predictions of the W and lightest Higgs bosons in the MRSSM and showed that agreement with experimental data is possible, in spite of tree-level shifts from violations of custodial symmetry and from mixing with other Higgs states, respectively.

Table 2 shows benchmark parameter points defined in that reference. They exemplify parameter regions in which m_W and m_{H_1} agree with experiment. They are characterized by large $|\Lambda| \approx 1$, rather light Dirac higgsinos and gauginos, and they have $\tan \beta = 3, 10, 40$, respectively.

For all three benchmark points the two-loop correction to m_{H_1} is around +5 GeV. As discussed in the previous sections, the largest part of this is due to the $\mathcal{O}(\alpha_t \alpha_s)$ corrections. The MRSSM-specific

	BMP1	BMP2	BMP3
$\tan \beta$	3	10	40
B_μ	500^2	300^2	200^2
λ_d, λ_u	1.0, -0.8	1.1, -1.1	0.15, -0.15
Λ_d, Λ_u	-1.0, -1.2	-1.0, -1.0	-1.0, -1.15
M_B^D	600	1000	250
$m_{R_u}^2$	2000^2	1000^2	1000^2
μ_d, μ_u		400, 400	
M_W^D		500	
M_O^D		1500	
m_T^2, m_S^2, m_O^2		$3000^2, 2000^2, 1000^2$	
$m_{Q;1,2}^2, m_{Q;3}^2$		$2500^2, 1000^2$	
$m_{D;1,2}^2, m_{D;3}^2$		$2500^2, 1000^2$	
$m_{U;1,2}^2, m_{U;3}^2$		$2500^2, 1000^2$	
m_L^2, m_E^2		1000^2	
$m_{R_d}^2$		700^2	
v_S	4.96	0.67	-0.30
v_T	-0.34	-0.20	-0.34
$m_{H_d}^2$	673^2	743^2	1160^2
$m_{H_u}^2$	-535^2	-542^2	-541^2
m_{H_1}	130.3 GeV	130.3 GeV	129.8 GeV
m_W	80.400 GeV	80.384 GeV	80.393 GeV
HiggsBounds's obsratio	0.67	0.68	0.67
HiggsSignals's p-value	0.03	0.03	0.03

Table 2: Benchmark points of Ref. [1]. Dimensionful parameters are given in GeV or GeV^2 , as appropriate. The first two parts define input parameters. The third part shows parameters derived from electroweak symmetry breaking after solving the tadpole equations at two loops. The last part gives the theory predictions for the Higgs boson mass at the two-loop level and further quantities relevant for comparison with experiment.

corrections of $\mathcal{O}(\alpha_\Lambda^2)$ are small since the values of Λ_u , though large, are still not as large as needed to make these corrections dominate, see Figs. 1, 2 for two out of three benchmarks. The magnitude of the total two-loop correction is consistent with the theory error estimate given in Ref. [1].

The upward shift of m_{H_1} implies that it is easier to obtain agreement with the measured value, i.e. smaller values of $|\Lambda_u|$ are sufficient. In Tab. 3 we provide new, slightly modified benchmark points, whose definitions differ only in the values of Λ_u . The two-loop Higgs boson mass prediction agrees well with experiment, and the good agreement of m_W with experiment is unchanged. Likewise, both the old and the new set of benchmark points pass checks against HiggsBounds [40–42] and HiggsSignals [43, 44].

In Fig. 6 we give an update to some of the subfigures from Figs. 4 and 5 of Ref. [1]. These show the predictions of m_W and m_{H_1} as contour lines in several two-dimensional parameter spaces. The Higgs boson mass is evaluated at the two-loop level. As discussed before, with the exception of the regions of very large Λ , there is a general positive contribution to the lightest Higgs boson mass between 4 and 5 GeV. Accordingly, the contour lines, in particular the central green region in which the Higgs boson mass agrees with experiment, shift to slightly lower values of Λ . Also, the overlap region, where Higgs and W boson masses agree with experiment, is enlarged.

	BMP1'	BMP2'	BMP3'
Λ_u	-1.11	-0.85	-1.03
v_S	5.2	1.01	-0.22
v_T	-0.25	-0.02	-0.21
$m_{H_d}^2$	674^2	764^2	1160^2
$m_{H_u}^2$	-502^2	-512^2	-516^2
m_{H_1}	125.3 GeV	125.5 GeV	125.4 GeV
m_W	80.397 GeV	80.381 GeV	80.386 GeV
HiggsBounds's obsratio	0.61	0.65	0.87
HiggsSignals's p-value	0.72	0.66	0.72

Table 3: Adapted benchmark points; other parameters are as given in Tab. 2

6 Conclusions

In this work we have presented the impact of two-loop corrections on the mass of the lightest Higgs boson in the MRSSM. The calculation has been performed using the framework of **SARAH** in the approximation of the vanishing electroweak gauge couplings and external momenta of the Higgs self energies. The code has been cross-checked with an analytic calculation of the most important new corrections. We have separately analyzed the impact of contributions involving the λ, Λ -couplings, which already appear in the one-loop corrections, and of the strong corrections involving gluon, Dirac gluino, and sgluon exchange.

In the previous work [1] and the present paper we have found that the lightest Higgs boson mass in the MRSSM differs from the one in the usual MSSM in several respects. At tree-level the additional mixing with additional scalar states reduces the MRSSM Higgs mass below the MSSM value. At the one-loop level, the top/stop contributions cannot be as large as in the MSSM, because stop mixing is forbidden by R-symmetry. However, the new contributions from the superpotential λ, Λ -terms have a similar structure as the top/stop contributions. If the λ, Λ -couplings are similar in magnitude to the top Yukawa coupling, the lightest Higgs boson mass can easily be in the ballpark of the experimentally allowed range.

The two-loop corrections governed by these λ, Λ -couplings, however, amount to only 1 GeV or less in parameter regions in which the Higgs boson mass agrees with experiment. The most important two-loop contributions are the strong corrections of $\mathcal{O}(\alpha_t \alpha_s)$. As we have shown the Dirac gluino and gluon contributions alone are very similar to the MSSM strong contributions for vanishing stop mixing. The inclusion of the sgluons changes the picture. The sgluon contributions are positive and rise with the Dirac gluino mass, such that the total $\mathcal{O}(\alpha_t \alpha_s)$ corrections of the MRSSM are larger than the ones of the MSSM, independently of the magnitude of stop mixing.

Overall, the MRSSM two-loop corrections to the lightest Higgs boson mass are typically positive. E.g. for the benchmark parameter points proposed in Ref. [1], the two-loop corrections to the Higgs boson mass amount to approximately +5 GeV, within the error estimate of that reference. Since perturbation theory shows a converging behavior and since the λ, Λ -corrections are subdominant (for $|\lambda|, |\Lambda|$ less than around 1.2), we estimate the remaining theory uncertainty to be not larger than the one of the MSSM.

The positive two-loop corrections make it easier to achieve agreement between the theory prediction for the lightest Higgs boson mass and the measured value. We have provided an update of the analysis of Ref. [1], showing parameter regions of simultaneous agreement of the Higgs and W boson mass predictions with experiment. Compared to Ref. [1], the allowed parameter regions are slightly larger and located at smaller values of the λ, Λ -couplings.

Acknowledgments

We would like to thank Kilian Nickel and Florian Staub for communication about SARAH. Work supported in part by the Polish National Science Centre grants under OPUS-2012/05/B/ST2/03306, DEC-2012/05/B/ST2/02597, the European Commission through the contract PITN-GA-2012-316704 (HIGGSTOOLS), the German DFG Research Training Group 1504 and the DFG grant STO 876/4-1.

References

- [1] P. Diessner, J. Kalinowski, W. Kotlarski, and D. Stöckinger, “Higgs boson mass and electroweak observables in the MRSSM,” *JHEP*, vol. 1412, p. 124, 2014.
- [2] G. Aad *et al.*, “Combined Measurement of the Higgs Boson Mass in pp Collisions at $\sqrt{s} = 7$ and 8 TeV with the ATLAS and CMS Experiments,” 2015.
- [3] R. Harlander, P. Kant, L. Mihaila, and M. Steinhauser, “Higgs boson mass in supersymmetry to three loops,” *Phys.Rev.Lett.*, vol. 100, p. 191602, 2008.
- [4] P. Kant, R. Harlander, L. Mihaila, and M. Steinhauser, “Light MSSM Higgs boson mass to three-loop accuracy,” *JHEP*, vol. 1008, p. 104, 2010.
- [5] T. Hahn, S. Heinemeyer, W. Hollik, H. Rzehak, and G. Weiglein, “High-Precision Predictions for the Light CP -Even Higgs Boson Mass of the Minimal Supersymmetric Standard Model,” *Phys.Rev.Lett.*, vol. 112, no. 14, p. 141801, 2014.
- [6] P. Draper, G. Lee, and C. E. M. Wagner, “Precise estimates of the Higgs mass in heavy supersymmetry,” *Phys.Rev.*, vol. D89, no. 5, p. 055023, 2014.
- [7] G. Degrandi, S. Di Vita, and P. Slavich, “Two-loop QCD corrections to the MSSM Higgs masses beyond the effective-potential approximation,” *Eur.Phys.J.*, vol. C75, no. 2, p. 61, 2015.
- [8] S. Borowka, T. Hahn, S. Heinemeyer, G. Heinrich, and W. Hollik, “Momentum-dependent two-loop QCD corrections to the neutral Higgs-boson masses in the MSSM,” *Eur.Phys.J.*, vol. C74, no. 8, p. 2994, 2014.
- [9] W. Hollik and S. Paßehr, “Two-loop top-Yukawa-coupling corrections to the Higgs boson masses in the complex MSSM,” *Phys.Lett.*, vol. B733, pp. 144–150, 2014.
- [10] W. Hollik and S. Paßehr, “Higgs boson masses and mixings in the complex MSSM with two-loop top-Yukawa-coupling corrections,” *JHEP*, vol. 1410, p. 171, 2014.
- [11] F. Staub, “Automatic Calculation of supersymmetric Renormalization Group Equations and Self Energies,” *Comput.Phys.Commun.*, vol. 182, pp. 808–833, 2011.
- [12] F. Staub, “SARAH 3.2: Dirac Gauginos, UFO output, and more,” *Comput.Phys.Commun.*, vol. 184, pp. pp. 1792–1809, 2013.
- [13] F. Staub, “SARAH 4: A tool for (not only SUSY) model builders,” *Comput.Phys.Commun.*, vol. 185, pp. 1773–1790, 2014.
- [14] W. Porod, “SPHeno, a program for calculating supersymmetric spectra, SUSY particle decays and SUSY particle production at $e^+ e^-$ colliders,” *Comput.Phys.Commun.*, vol. 153, pp. 275–315, 2003.
- [15] W. Porod and F. Staub, “SPHeno 3.1: Extensions including flavour, CP-phases and models beyond the MSSM,” *Comput.Phys.Commun.*, vol. 183, pp. 2458–2469, 2012.

- [16] P. Athron, J.-h. Park, D. Stöckinger, and A. Voigt, “FlexibleSUSY – A spectrum generator generator for supersymmetric models,” *Comput.Phys.Commun.*, vol. 190, pp. 139–172, 2015.
- [17] B. Allanach, “SOFTSUSY: a program for calculating supersymmetric spectra,” *Comput.Phys.Commun.*, vol. 143, pp. 305–331, 2002.
- [18] P. Fayet, “Supergauge Invariant Extension of the Higgs Mechanism and a Model for the electron and Its Neutrino,” *Nucl.Phys.*, vol. B90, pp. 104–124, 1975.
- [19] A. Salam and J. Strathdee, “Supersymmetry and Fermion Number Conservation,” *Nucl.Phys.*, vol. B87, p. 85, 1975.
- [20] G. D. Kribs, E. Poppitz, and N. Weiner, “Flavor in supersymmetry with an extended R-symmetry,” *Phys.Rev.*, vol. D78, p. 055010, 2008.
- [21] W. Buchmuller and D. Wyler, “CP Violation and R Invariance in Supersymmetric Models of Strong and Electroweak Interactions,” *Phys.Lett.*, vol. B121, p. 321, 1983.
- [22] M. R. Buckley, D. Hooper, and J. Kumar, “Phenomenology of Dirac Neutralino Dark Matter,” *Phys.Rev.*, vol. D88, p. 063532, 2013.
- [23] E. J. Chun, J.-C. Park, and S. Scopel, “Dirac gaugino as leptophilic dark matter,” *JCAP*, vol. 1002, p. 015, 2010.
- [24] G. Belanger, K. Benakli, M. Goodsell, C. Moura, and A. Pukhov, “Dark Matter with Dirac and Majorana Gaugino Masses,” *JCAP*, vol. 0908, p. 027, 2009.
- [25] P. J. Fox, A. E. Nelson, and N. Weiner, “Dirac gaugino masses and supersoft supersymmetry breaking,” *JHEP*, vol. 0208, p. 035, 2002.
- [26] T. Plehn and T. M. Tait, “Seeking Sgluons,” *J.Phys.*, vol. G36, p. 075001, 2009.
- [27] S. Choi, M. Drees, J. Kalinowski, J. Kim, E. Popena, *et al.*, “Color-Octet Scalars of N=2 Supersymmetry at the LHC,” *Phys.Lett.*, vol. B672, pp. 246–252, 2009.
- [28] S. Choi, D. Choudhury, A. Freitas, J. Kalinowski, J. Kim, *et al.*, “Dirac Neutralinos and Electroweak Scalar Bosons of N=1/N=2 Hybrid Supersymmetry at Colliders,” *JHEP*, vol. 1008, p. 025, 2010.
- [29] S. Choi, D. Choudhury, A. Freitas, J. Kalinowski, and P. Zerwas, “The Extended Higgs System in R-symmetric Supersymmetry Theories,” *Phys.Lett.*, vol. B697, pp. 215–221, 2011.
- [30] K. Benakli, M. D. Goodsell, and F. Staub, “Dirac Gauginos and the 125 GeV Higgs,” *JHEP*, vol. 1306, p. 073, 2013.
- [31] G. Aad *et al.*, “Search for pair-produced massive coloured scalars in four-jet final states with the ATLAS detector in proton-proton collisions at $\sqrt{s} = 7$ TeV,” *Eur.Phys.J.*, vol. C73, no. 1, p. 2263, 2013.
- [32] ATLAS Collaboration, “Search for anomalous production of events with same-sign dileptons and b jets in 14.3 fb^{-1} of pp collisions at $\sqrt{s} = 8$ TeV with the ATLAS detector,” ATLAS-CONF-2013-051, 2013.
- [33] W. Kotlarski, A. Kalinowski, and J. Kalinowski, “Searching for Sgluons in the Same-sign Leptons Final State at the LHC,” *Acta Phys.Polon.*, vol. B44, no. 11, pp. 2149–2154, 2013.
- [34] E. Bertuzzo, C. Frugiuele, T. Gregoire, and E. Ponton, “Dirac gauginos, R symmetry and the 125 GeV Higgs,” 2014.

- [35] M. D. Goodsell, K. Nickel, and F. Staub, “Two-Loop Higgs mass calculations in supersymmetric models beyond the MSSM with SARAH and SPheno,” *Eur.Phys.J.*, vol. C75, no. 1, p. 32, 2015.
- [36] W. Hollik and D. Stöckinger, “MSSM Higgs-boson mass predictions and two-loop non-supersymmetric counterterms,” *Phys.Lett.*, vol. B634, pp. 63–68, 2006.
- [37] H. K. Dreiner, K. Nickel, and F. Staub, “On the two-loop corrections to the Higgs mass in trilinear R-parity violation,” *Phys.Lett.*, vol. B742, pp. 261–265, 2015.
- [38] M. D. Goodsell, K. Nickel, and F. Staub, “Two-loop corrections to the Higgs masses in the NMSSM,” *Phys.Rev.*, vol. D91, no. 3, p. 035021, 2015.
- [39] S. P. Martin, “Two loop effective potential for a general renormalizable theory and softly broken supersymmetry,” *Phys.Rev.*, vol. D65, p. 116003, 2002.
- [40] P. Bechtle, O. Brein, S. Heinemeyer, G. Weiglein, and K. E. Williams, “HiggsBounds: Confronting Arbitrary Higgs Sectors with Exclusion Bounds from LEP and the Tevatron,” *Comput.Phys.Commun.*, vol. 181, pp. 138–167, 2010.
- [41] P. Bechtle, O. Brein, S. Heinemeyer, G. Weiglein, and K. E. Williams, “HiggsBounds 2.0.0: Confronting Neutral and Charged Higgs Sector Predictions with Exclusion Bounds from LEP and the Tevatron,” *Comput.Phys.Commun.*, vol. 182, pp. 2605–2631, 2011.
- [42] P. Bechtle, O. Brein, S. Heinemeyer, O. Stål, T. Stefaniak, *et al.*, “HiggsBounds – 4: Improved Tests of Extended Higgs Sectors against Exclusion Bounds from LEP, the Tevatron and the LHC,” *Eur.Phys.J.*, vol. C74, no. 3, p. 2693, 2014.
- [43] P. Bechtle, S. Heinemeyer, O. Stål, T. Stefaniak, and G. Weiglein, “HiggsSignals: Confronting arbitrary Higgs sectors with measurements at the Tevatron and the LHC,” *Eur.Phys.J.*, vol. C74, no. 2, p. 2711, 2014.
- [44] P. Bechtle, S. Heinemeyer, O. Stål, T. Stefaniak, and G. Weiglein, “Probing the Standard Model with Higgs signal rates from the Tevatron, the LHC and a future ILC,” *JHEP*, vol. 1411, p. 039, 2014.